Absence of a ''Threshold Effect'' in the Energy Loss of Slow Protons Traversing Large-Band-Gap Insulators

K. Eder, D. Semrad, and P. Bauer
Institut für Experimentalphysik, Johannes-Kepler Universität Linz, A-4040 Linz, Austria

R. Golser
Institut für Radiumforschung und Kernphysik, Universität Wien, A-1090 Wien, Austria

P. Maier-Komor
Target Laboratory, Technical University Munich, D-85748 Garching, Germany

F. Aumayr
Institut für Allgemeine Physik, Technische Universität Wien, A-1040 Wien, Austria

M. Peñalba
Departamento de Física Aplicada I, E.T.S.I.I. y T., Universidad del País Vasco, Bilbao, Spain

A. Arnau, J. M. Ugalde, and P. M. Echenique
Departamento de Física de Materiales, Universidad del País Vasco, Apartado 1072, San Sebastián 20080, Spain
(Received 1 July 1997)

The electronic stopping cross section ε of slow hydrogen projectiles in large-band-gap insulators has been measured at energies of a few keV. Even at velocities as low as $v_0/3$ ($v_0 = c/137$), we find no influence of the band gap on the velocity dependence of ε, contrary to the case of gaseous targets with similar minimum excitation energy. The magnitude of ε and its essentially linear velocity dependence allow us to arrive at the following conclusion: Electron promotion processes contribute substantially to stopping due to formation of molecular orbitals. This points towards the existence of a bound electron state at a proton that moves slowly in an insulator. A simple model based on the calculation of molecular orbital correlation diagrams for the H/LiF collision system supports the idea of local reduction of the band gap of an insulating target. [S0031-9007(97)04585-7]

PACS numbers: 34.50.Bw, 78.90.+t, 79.20.–m, 79.90.+b

The electronic stopping power $-dE/dx$ of light ions at low velocities (i.e., H and He ions with velocities v lower than the Bohr velocity $v_0 = c/137$) is widely assumed to be proportional to the ion velocity. Both electron gas descriptions of the valence electrons of a metallic target and semiclassical models that treat collisions between atoms arrive at the result [1,2]

$$-dE/dx \propto v\,. \tag{1}$$

In the case of metallic targets the dominant mechanism for slow ions to lose energy is electron hole pair creation at the Fermi level, while in the case of atom-atom collisions the dominant channel is capture and loss of electrons. Consequently, no matter whether the target is a metallic solid [3] or a gas [4], most experiments confirm Eq. (1). A spectacular exception has been reported recently for stopping of slow protons in He [5] and to less extent in Ne [6], which has been explained by the large threshold in the excitation spectrum in these noble gases [7].

The energy gap E_g of a solid insulator may be as large as the minimum excitation energies of noble gas atoms, hence a similar threshold effect for proton stopping could be expected. Thus, quite fundamental information may be obtained from the investigation of the stopping of very slow protons in insulators. We address this problem by investigating the electronic stopping of slow H projectiles in large-band-gap insulators both experimentally and theoretically.

The energy loss measurements were performed in transmission geometry using the ECR ion source [8] at the TU Wien and the time-of-flight (TOF) setup LISA [5,6]. We chose protons and deuterons of 2–10 keV as projectiles and polycrystalline alumina (Al_2O_3, $E_g \approx 8$ eV), silica (SiO_2, $E_g \approx 8$ eV) and lithiumfluoride (LiF, $E_g \approx 14$ eV) as target materials. Self-supporting carbon foils of 2.8 $\mu g/cm^2 \pm 5\%$ [9] were partly covered by a thin evaporated layer of the insulator (2 to 4 $\mu g/cm^2$). The thickness of the films was determined by a quartz crystal thickness monitor (± 0.1 $\mu g/cm^2$) with an uncertainty due to different positions of the target and the quartz. In the case of LiF targets we also used Rutherford backscattering (RBS) of 600 keV deuterons for thickness determination. Both results for the thickness of LiF relative to that of carbon agreed within the statistical uncertainties ($\pm 20\%$).

In order to minimize electronic sputtering which is the main erosion process for LiF [10], the ion dose for the RBS

 0031-9007/97/79(21)/4112(4)$10.00

measurements was kept low ($<3 \times 10^{14}$ ions/cm^2). Indeed no loss of LiF was observed during accumulation of the RBS spectra. Although electronic stopping is somewhat more efficient at low energy, we expect even less erosion during our TOF experiments, since the total ion fluence was much less (10^{12} ions/cm^2). This is corroborated by the fact that we obtained concordant results for different target thicknesses (see Fig. 2) and also on one target with ions of the same velocity (see the data point at 2.9 keV) in independent runs on different days (within a period of one and a half months). The measured energy resolution of the TOF assembly was about 0.1%. The TOF spectrum of a single target shows two peaks: one that arises from projectiles traversing carbon plus insulator and one from traversing carbon alone. After converting the TOF spectra to energy spectra, the difference in the centers of gravity of these two peaks yields the energy loss ΔE in the insulator. From ΔE and the target thickness in terms of atoms per unit area, nd, the stopping cross section ε is obtained as $\varepsilon(\bar{v}) = \Delta E/nd$ with $\bar{v} = (v_{\text{in}} + v_{\text{out}})/2$, v_{in} and v_{out} being the mean velocity of particles entering and exiting the target, respectively. The total error of ε is about 7%, mainly due to uncertainties in the target thickness and errors in the determination of the centers of gravity. The influence of multiple scattering (increase in path length and nuclear energy losses) was corrected by using TRIM [11]; the correction was 3% at most.

In Fig. 1 we present the stopping cross section per molecule for the oxides Al_2O_3 and SiO_2. First of all, we notice that at low velocities ε is nicely proportional to v as indicated by the dashed lines, without any indication of a threshold effect [7]. Second, we find a ratio $\varepsilon_{Al_2O_3}/\varepsilon_{SiO_2} = 1.5$ just the same as at higher energies [12]. This may become evident by the fact that at low velocities the number of electrons in the valence bands determines the stopping behavior. Band structure calculations show that the uppermost valence band arises from O $2p$ nonbonding orbitals forming the familiar O_2^- ion. It contains 18 electrons in Al_2O_3 and 12 electrons in SiO_2 [13]. In Fig. 1 we also compare the data to linear dielectric theory for Al_2O_3 using the dielectric function from Ref. [14]. While excellent agreement between theory and experiment is obtained for energies at and above the stopping maximum, the theory strongly underestimates the experimental data at low energies. Whereas for metals linear theory is assumed to be correct within a factor of 1.5 [2], the huge discrepancy found for oxides at low energies demonstrates that linear theory misses the dominant contribution to ε.

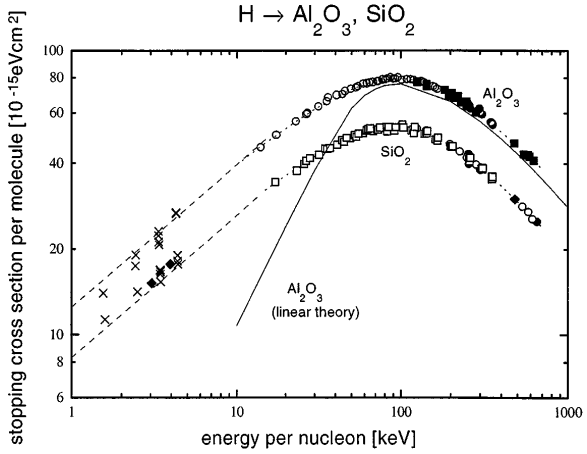

FIG. 1. Measured stopping cross sections per molecule of alumina and silica for protons and deuterons as a function of the energy per nucleon E/A of the projectiles. These measurements are represented by crosses (×) and diamonds (◆) and the data from Ref. [11] by circles (●, ○) and squares (■, □). The full line represents the result of theory for alumina (see text), the dashed lines are proportional to velocity, and the dotted lines are fits to the high energy data.

In Fig. 2 we present ε per molecule for LiF together with the corresponding data for Ne [6]. We find the following results: First, ε_{LiF} also is nicely proportional to velocity, and second, ε_{LiF} exceeds ε_{Ne} by a factor of 3 to 4. This is unexpected, because the energy gap of LiF and the minimum excitation energy of Ne are similar in magnitude. These findings cannot be explained in terms of Coulomb excitation of the target electrons by a bare proton [7] but call for an additional energy loss channel at low velocities.

Considering the processes that may contribute to the energy loss in insulators, we first look at projectile inelastic processes [15] (capture and loss of electrons leading to ε_{CL}). In our energy regime the cross section for electron capture σ_{capt} is much larger than that of electron loss σ_{loss}.

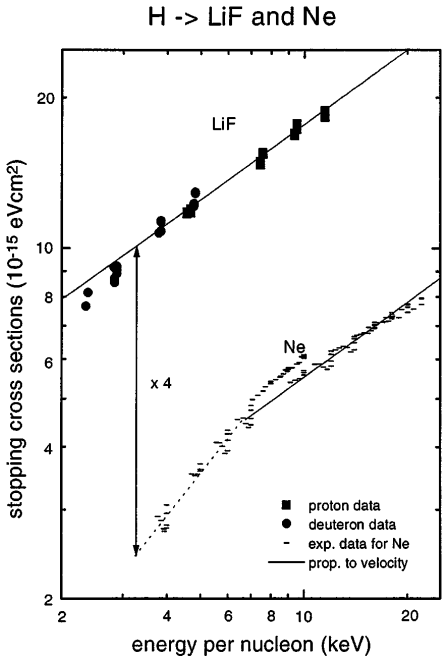

FIG. 2. Measured stopping cross section per molecule of LiF for protons (■) and deuterons (●) as a function of the energy per nucleon E/A of the projectiles. For comparison, we also show the experimental results of Ne (−) from [6].

Thus, ε_{CL} may be estimated as $\varepsilon_{CL} \approx \sigma_{loss}(E_b + E_{kin})$, where E_b is the binding energy of the electron in the target atom and E_{kin} is the kinetic energy of the electron moving with the velocity of the proton. In order to explain the difference between the LiF data and the Ne data by projectile inelastic processes we would have to postulate σ_{loss} of LiF to be 6 times as large as σ_{loss} of Ne. This is in clear contradiction to the fact that for both systems close collisions are needed to transfer the large amount of energy needed to ionize the projectile. Consequently, we conclude that the contribution of ε_{CL} is too small to explain our experimental findings. In the following, we introduce electron promotion as the relevant mechanism.

Electron promotion may take place when molecular orbitals (MO) evolve as projectile and target atoms approach each other and their electron wave functions overlap. MO promotion can provide a mechanism to raise an electron from a bound level of the LiF crystal to an unoccupied state even by a rather distant collision (a few a.u.). This overlap is expected to be much more pronounced for LiF as compared to Ne, due to the larger ionic radius of the F^- centers of the LiF ionic crystal. Insight into the MO promotion in slow collisions is gained by analyzing the energy levels of molecular orbitals as a function of the distance of the colliding partners [16]. At large distances, the MOs asymptotically merge into the atomic states. For ionic crystal targets, the effect of the environment of the anion must be taken into account.

Therefore, we have modeled the F^- by a fluorine anion positioned at an octahedron center and surrounded by six positive unit charges. The distances have been fixed so that we get the correct value of the Madelung potential of the fcc lattice at the F^- center. This simple model is not able to reproduce the electronic structure of LiF, of course, but accounts for the basic physics to explain qualitatively low energy stopping. The energy gap E_g is associated with the difference between the energy of the highest occupied MO (HOMO) that correlates with the atomic $2p$ state of F^- and of the lowest unoccupied MO (LUMO). Our model gives $E_g = 9.5$ eV (as compared to 14 eV from literature). In Fig. 3 we plot the energies of the MOs that develop as H approaches F^- with zero impact parameter on a trajectory normal to the "crystal" surface, as a function of the H-F^- separation (we find no noticeable change for a nonperpendicular approach). All calculations have been done with the GAUSSIAN94 suite of programs [17]. Both Hartree-Fock and configuration interaction with only single excitation (CIS) calculations have been carried out. We used the 6-31 + $G(d, f)$ basis set which includes one diffuse basis function to properly account for the loosely bound outer electrons. The CIS wave function is needed to relate the energy of the virtual orbital with the excitation energies of the system [18,19]. As mentioned before, the minimum electron excitation energy for MO promotion of one electron from the HOMO to the LUMO represents our estimate of E_g in the ionic crystal.

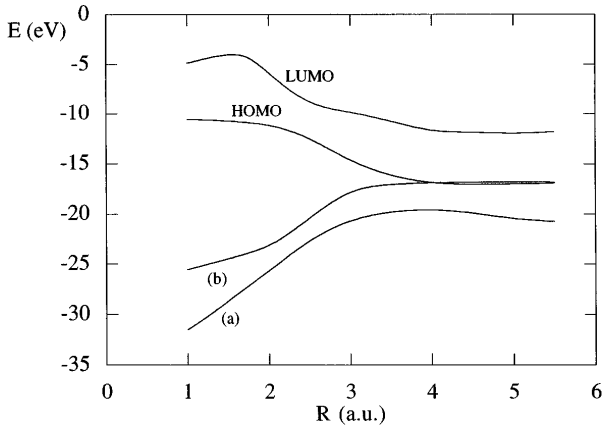

FIG. 3. Molecular orbital (MO) energy levels (in eV) of the HF^- system as a function of the distance between the two atoms, R, in a.u. A positive distribution of charges has been included to give the correct value of the Madelung potential at the F position (11 eV). The curve labeled HOMO is the highest occupied molecular orbital and the one labeled LUMO is the lowest unoccupied molecular orbital. The MO represented by curve (a) can be identified at long distances with the $1s$ orbital of H, while the ones represented by (b) and by HOMO asymptotically correlate with the $2p$ orbital of F^-. Note that at $R \approx 2.5$ a.u. the energy distance between HOMO and LUMO is only 4 eV.

We find a significant local reduction of the band gap, by about a factor of 2 with respect to the undisturbed crystal, even at distances of 5 a.u. When the distance between H and F^- is between 2 and 3 a.u. the calculated energy gap is reduced to about 4 eV. Similar effects have been reported [20] for Tl^+ substitutional impurities in ionic crystals. Very recently, the emission of energetic secondary electrons from a LiF surface under bombardment by slow protons has been explained in terms of MO processes [21]. Concerning electronic stopping, the local reduction of the band gap provides an effective energy loss channel even for keV hydrogen projectiles. By way of contrast, this MO process is not expected to contribute to the stopping in Ne gas, except for very close—and therefore unlikely—collisions. Qualitatively, the oxides should behave the same way, due to the partially ionic character of their chemical bonds where the negative O ion plays the role of F^- in the fluoride.

In conclusion, we have found that the electronic stopping of large band gap insulators (Al_2O_3, SiO_2, and LiF) for keV protons does not show any threshold effect, contrary to the case of gaseous targets with similar minimum excitation energies like Ne or He. Based on an analysis of the MO correlation diagram for the H-LiF system, the MO promotion mechanism is introduced as the dominant channel for the energy loss. We note that the contribution of MO processes calls for the existence of a bound electron state at the proton moving through the insulator. The local reduction of the band gap that we find for the H-LiF system means that large band gap insulators keep

their properties when interacting with electrons but are so strongly perturbed by slow hydrogen projectiles that, as far as electronic stopping is concerned, they no longer behave like an insulator in the conventional sense.

This work has been partly supported by the Austrian Fonds zur Förderung der Wissenschaftlichen Forschung under Contracts No. P10183-PHY and No. P10740-PHY. Support by the European Community within the Human Capital and Mobility Program, Project No. ERBCHRXTC 94.0479, is gratefully acknowledged. Some of us (M. P., A. A., J. M. U., and P. M. E.) gratefully acknowledge financial support by Eusko Jaurlaritza, Gipuzkoako Foru Aldundia, Euskal Herriko Unibertsitatea and the Spanish D.G.I.C.Y.T. The authors thank Arend Niehaus for helpful suggestions in the early stage of this work.

[1] J. Lindhard, K. Dan. Vidensk. Selsk. Mat.-Fys. Medd. **28**, No. 8 (1954); R. H. Ritchie, Phys. Rev. **114**, 644 (1959).
[2] P. M. Echenique, R. M. Nieminen, and R. H. Ritchie, Solid State Commun. **37**, 779 (1981).
[3] J. E. Valdés, J. C. Eckardt, G. H. Lantschner, and N. R. Arista, Phys. Rev. A **49**, 1083 (1994).
[4] V. Dose and G. Sele, Z. Phys. A **272**, 237 (1975).
[5] R. Golser and D. Semrad, Phys. Rev. Lett. **66**, 1831 (1991).
[6] A. Schiefermueller, R. Golser, R. Stohl, and D. Semrad, Phys. Rev. A **48**, 4467 (1993).
[7] D. Semrad, Phys. Rev. A **33**, 1646 (1986).
[8] M. Leitner, D. Wutte, J. Brandstötter, F. Aumayr, and HP. Winter, Rev. Sci. Instrum. **65**, 1091 (1994).
[9] P. Maier-Komor, G. Dollinger, and E. Hammann, Nucl. Instrum. Methods Phys. Res., Sect. A **303**, 88 (1991).
[10] T. Neidhart, Z. Toth, M. Hochhold, M. Schmid, and P. Varga, Nucl. Instrum. Methods Phys. Res., Sect. B **90**, 496–500 (1994).
[11] J. F. Ziegler, J. P. Biersack, and U. Littmark, *The Stopping and Range of Ions in Solids* (Pergamon, New York, 1985), Vol. 1.
[12] P. Bauer, R. Golser, F. Aumayr, D. Semrad, A. Arnau, E. Zarate, and R. Diez-Muiño, Nucl. Instrum. Methods Phys. Res., Sect. B (to be published); P. Bauer, W. Rössler, and P. Mertens, Nucl. Instrum. Methods Phys. Res., Sect. B **69**, 46 (1992).
[13] R. H. French, J. Am. Ceram. Soc. **73**, 477 (1990).
[14] A. Arnau, P. M. Echenique, and R. H. Ritchie, Nucl. Instrum. Methods Phys. Res., Sect. B **33**, 138 (1988); I. Paulini, W. Heiland, A. Arnau, E. Zarate, and P. Bauer, Nucl. Instrum. Methods Phys. Res., Sect. B **114**, 39 (1996).
[15] A. Arnau, M. Peñalba, P. M. Echenique, and F. Flores, Nucl. Instrum. Methods Phys. Res., Sect. B **69**, 102 (1992).
[16] R. Souda *et al.*, Phys. Rev. B **50**, 18 489 (1994).
[17] M. J. Frisch *et al.*, GAUSSIAN 94/DFT (Revision A.1), Gaussian Inc., Pittsburgh, PA, 1995.
[18] N. Björnå, J. Phys. B **6**, 1412 (1973).
[19] S. Huzinaga and C. Arnau, Phys. Rev. A **1**, 1285 (1970).
[20] M. Berrondo and J. F. Rivas-Silva, Int. J. Quantum Chem. **29**, 253 (1995).
[21] P. Stracke, F. Wiegershaus, S. Krischok, V. Kempter, P. A. Zeijlmans van Emmichoven, A. Niehaus, and F. J. García de Abajo, Nucl. Instrum. Methods Phys. Res., Sect. B **125**, 67 (1997).